Archaeological and Anthropological Sciences (2020) 12: 267
https://doi.org/10.1007/s12520-020-01227-7

ORIGINAL PAPER

# The transition of alkaline flux of ancient Chinese faience beads (1046–476 BC): a case study on the samples from Pingdingshan, Henan province

Junqing Dong[1,2] · Yongqing Hu[3] · Song Liu[1] · Qinghui Li[1,2]

Received: 11 June 2020 / Accepted: 15 October 2020 / Published online: 24 October 2020


## Abstract

Eleven faience objects unearthed from cemeteries (1046–476 BC) of the Zhou Dynasty in Pingdingshan, Henan province, China, were characterized by scanning electron microscopy–energy dispersive X-ray spectrometry. The analysis results provided information on the chemical composition and microstructure of the faience objects, and conclusions were drawn regarding the forming and glazing methods, as well as the related glazing materials. Soda-rich, potash-rich, and mixed-alkali fluxes, as well as the cementation and efflorescence glazing methods, were utilized in forming these faience objects. Conventionally, a glazing mixture was applied to the quartz body, probably to strengthen it for handling prior to firing. In combination with the published data on other Chinese faience objects, it was possible to suggest the provenances, transition of the alkaline flux with time, and product and technology exchanges of the faience objects from Central China during the Zhou Dynasty (1046–221 BC). The soda-rich faience objects were imported from the West and were later replaced with the mixed-alkali faience ones since the middle Western Zhou Dynasty (976–878 BC). Since the early Western Zhou Dynasty (1046–977 BC), Chinese native potash-rich faience had been produced in the Zhou realm. This study will provide some insights into the technology exchange and origin of the potash-rich and mixed-alkali faience objects unearthed in China.

**Keywords** SEM–EDS · Chinese faience · Ying State cemetery · Production technology · Alkaline flux

## Introduction

Faience is generally known as nonclay silicate artifact that consists of a quartz sand and ground quartz body, bonded together by varying amounts of a glass phase and coated with a glaze. The earliest faience was produced in the Near East and Egypt during the 4th millennium BC and, subsequently, in the Indus Valley about 3rd millennium BC ago (Tite and Shortland 2008). Conversely, the first evidence of Chinese faience was found at Adunqiaolu (3330 ± 30 BC), an early Bronze Age site in Xinjiang, western China (Wang et al. 2020). Sometime toward the middle of the eleventh century BC, many faience objects appeared in the Yellow River Basin, for example, the Yujiawan site in the Gansu province (Wang et al. 2020) and the Ying State cemetery in the Henan province (Henan Provincial Institute of Cultural Relics and Archaeology and Pingdingshan Administration of Cultural Relics 2012; Dong et al. 2016). These objects were widespread in Central China (Zhou realm), including in the Shaanxi, Shanxi, and Henan provinces, during the Western Zhou Dynasty (1046–771 BC), and across regions of the Yangtze River Basin, including Hubei, Jiangsu, and Sichuan provinces (Gu 2015; Wang 2019). In recent decades, many scholars have analyzed the Chinese faience objects, including those imported and those produced in ancient China.

**Electronic supplementary material** The online version of this article (https://doi.org/10.1007/s12520-020-01227-7) contains supplementary material, which is available to authorized users.

✉ Qinghui Li
qinghuil@sina.com

[1] Sci-Tech Archaeology Center, Laboratory of Micro-Nano Optoelectronic Materials and Devices, Key Laboratory of Materials for High-Power Laser, Shanghai Institute of Optics and Fine Mechanics, Chinese Academy of Sciences, Shanghai 201800, China

[2] Center of Materials Science and Optoelectronics Engineering, University of Chinese Academy of Sciences, Beijing 100049, China

[3] Henan Provincial Institute of Cultural Relics and Archaeology, Zhengzhou 450000, China

Significant progress has been achieved in the research on the faience objects unearthed from the Yellow River Basin and western China using multi-techniques, such as scanning electron microscopy (SEM) with energy dispersive X-ray spectrometry (EDS), particle-induced X-ray emission (PIXE), X-ray fluorescence (XRF), X-ray diffraction (XRD), and Raman spectroscopy techniques. The related aspects included the determination of the alkaline flux (Brill et al. 1989; Liu et al. 2019; Lei and Xia 2015; Zhao et al. 2011), lead isotope analysis (Wang 1986; Brill et al. 1991), distribution area (Hou 1987; Li et al. 2009), production technology (Gu et al. 2014; Lei and Xia 2015; Liu et al. 2017; Wang et al. 2017; Wang et al. 2020); origin (Lin et al. 2019), and provenance and spread (Lei and Xia 2015; Wang et al. 2020; Yang 2020). In addition, replication processes have been attempted in the laboratory using the direct application glazing method for imitating ancient faience beads (Qin et al. 2012). Based on the results obtained from the laboratory replication experiments and the microstructural and compositional data from SEM–EDS, a typical western faience can be glazed using application, cementation, and efflorescence methods, particularly for large faience objects. In China, however, the overwhelming majority of faience artifacts are small beads and tubes, except for only a few *jue* objects (a kind of penannular ring, commonly made of jade) (Wang 2019).

For the study of the loss of the alkaline flux of faience objects caused by weathering, surface analytical techniques, such as portable XRF and PIXE, are not suitable because they cannot effectively determine the original concentrations of the alkaline fluxes (Dong et al. 2016; Li et al. 2009; Gu et al. 2014; Liu et al. 2017). In contrast, SEM and computed tomography (CT), which are widely used in material analysis (Zhang et al. 2015) and biomedicine (Jiang et al. 2008; Xia et al. 2018) to obtain detailed cross-sectional information. SEM–EDS is a very useful technique for studying both the flux and production technology of ancient faience objects. In recent years, Gu et al. (Gu 2015; Gu et al. 2014) and Liu et al. (2017) proposed a new method for studying the forming and glazing methods of Chinese faience objects by synchrotron radiation micro-CT (SR-μCT), although this method could not give the micro-area chemical composition information.

Despite decades of research on ancient Chinese faience, many questions still need to be further investigated, for instance, the provenances of the potash-dominated faience, the relationship between the mixed-alkali and the potash-rich faience objects unearthed in China, the admixture recipes for the quartz body, and forming technology. In fact, in previous studies, some mistakes were made in distinguishing the quartz-free glaze layer from the interaction layer. To better investigate the origin, development, and technology exchange of Chinese faience objects, it is necessary to research ancient faience objects from the same region or one site that has a long-lasting history.

## Archeological background

In the present project, we analyze the faience beads and tubes unearthed from the Zhou Dynasties tombs (1046–476 BC) in Pingdingshan, Henan province by SEM–EDS; furthermore, we discuss the alkaline flux, possible provenances, production technology, recipes, and the origin of the Chinese native faience objects in combination with previous published data.

The cemetery of the Ying State in Pingdingshan is located on at the Beizhi village (about E 113° 7′ 55.2″, N 33° 46′ 19.2″), Zhiyang town, Xinhua district, Pingdingshan city, Henan province, Central China. The cemetery is mainly occupied by tombs belonging to the aristocrats of the Ying State dated to the Western and Eastern Zhou Dynasties (1046–221 BC), as well as some common tombs of the Western and Eastern Han Dynasties (202 BC–220 AD). The cemetery was firstly discovered in 1979, and the archeological excavation began in 1986 and ended in 2007. Over 500 tombs were discovered during the excavation, and more than 10,000 objects were unearthed. The owners of nearly 20 tombs are the kings of the Ying State and their wives. The unearthed objects include bronze ritual vessels, potteries, weapons, chariots, and many exquisite necklaces and ornaments composed of jade, faience, carnelian, and clamshell or bone. Considering its significance in academic research, this cemetery was nominated as one of the greatest archeological discoveries of China in 1996 (Henan Provincial Institute of Cultural Relics and Archaeology and Pingdingshan Administration of Cultural Relics 2012).

Abundant blue–green faience beads and tubes were unearthed from several tombs in the Ying State cemetery dated from the early Western Zhou Dynasty to the early Spring and Autumn period (around 1046–665 BC); many of them had undergone weathering or were broken into fragments. Figure 1 shows the numbers of tombs and faience objects dated to different periods. Only 11 faience beads were found in tomb No. 231, indicating that these objects were very rare in the early Western Zhou Dynasty (1046–977 BC). The faience beads, together with carnelian and turquoise beads, form ornament sets (Fig. 2a). The numbers of both the faience objects and tombs increased obviously during the middle Western Zhou Dynasty (976–892 BC). Up to 2069 faience beads and tubes were unearthed from seven tombs, the owners of which included the marquises of Ying (Yinghou, 应侯) to the lowest aristocracy (Shi, 士); for instance, 1106 faience objects were found in just one tomb of a marquis' young wife. In those periods, faience was used to make the combined jade ornament neck sets (Fig. 2b) and jade pendant sets (Fig. 2c). A total of 119 faience artifacts were unearthed from the tombs of three aristocracies of the late Western Zhou Dynasty (877–771 BC). The typical faience tubes used as jade pendants are shown in Fig. 2d. In addition, 224 faience beads and tubes were excavated from the tomb of a senior aristocrat's wife of the early Spring and Autumn period (771–665 BC).

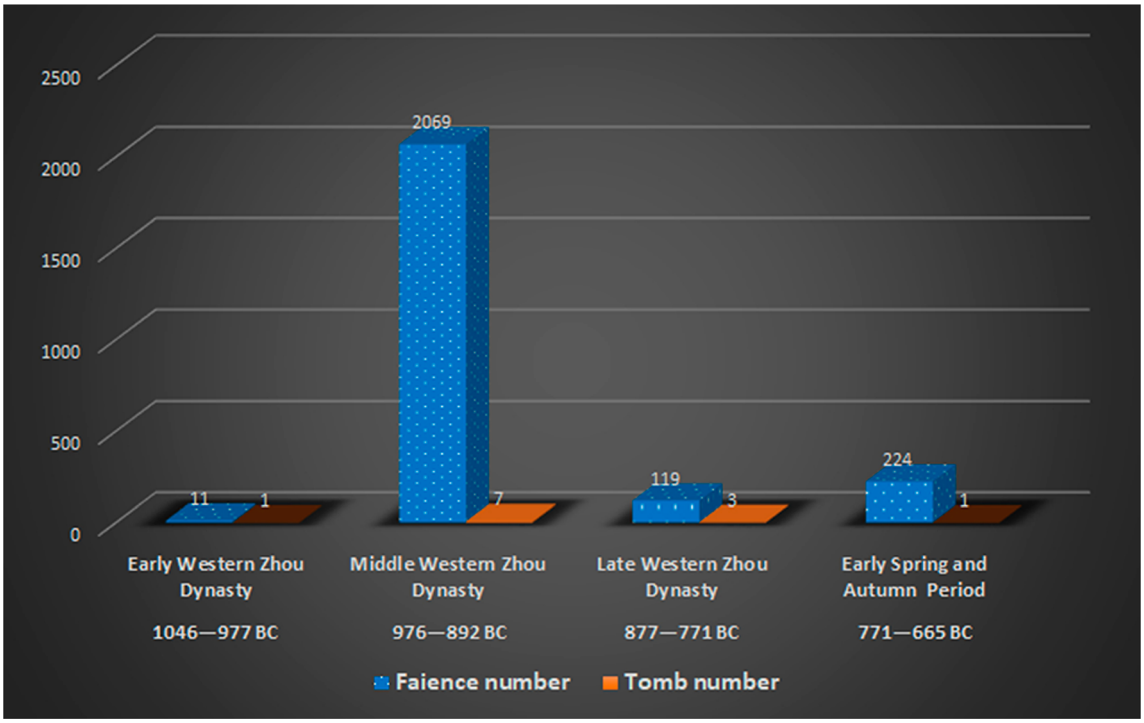


**Fig. 1** Bar chart of the faience objects and the tombs of different periods in the Ying State cemetery, Pingdingshan

## Samples

In the current study, we selected fragments from 10 faience beads and tubes unearthed from the Ying State cemetery of the above four periods for examination and analysis by SEM–EDS. In addition, for comparative study, we examined the fragment from a blue faience bead unearthed from the tomb of a king of the Xu State (Xulinggong) (Cultural Heritage Bureau of Pingdingshan City and Cultural Heritage Bureau of Ye County 2007) dated to the late Spring and Autumn period (~ 547 BC). The photographs and archeological information of the 11 samples are given in Fig. 3 and Table 1, respectively.

## Analytical methods

The samples were embedded with epoxy resin and polished with diamond paste down to a thickness of 1 μm to obtain a flat surface. Microscopic analyses and the elemental distribution analysis of two gold-coated samples (PY57-2 and YJ152-1) were also conducted using a COXEM EM-30PLUS scanning electron microscope equipped with an Oxford X-act compact 1414 EDS at Shanghai Opton Instrument Co., Ltd. Quantitative chemical analyses and EDS mappings were conducted at an accelerating voltage of 20 kV. Chemical components of the samples were established by no-standard quantitative analysis using the Oxford AZtecONE micro-analysis software. All the carbon-coated samples were analyzed to observe the microstructure in back-scatter electron (BSE) images; the chemical composition of the body and the interparticle vitreous phase of the samples were determined by SEM (TESCAN VEGA3 XMU) with EDS (Bruker Nano Gmbh 610 M) at the Chinese Academy of Cultural Heritage, University of Science and Technology Beijing. Quantitative chemical analyses were conducted at an accelerating voltage of 15 kV and a beam current of 20 μA. A focused 5-μm beam was used to avoid the analysis (at least horizontally) of the quartz particles near the glass. The concentration of each component was determined with a standard-less PB ZAF using the Bruker ESPRIT 2 micro-analysis software. The accuracy of the results was monitored by repeated analysis of Corning B, C, and D glass standards (see Table 3).

# Results and discussion

## Microstructures and production technologies

The microstructures (Figs. 4, 5, 7, and 8) and chemical composition (Tables 2 and 3) of the faience beads and tubes were elucidated by SEM–EDS. The test results of the Corning B, C, and D glass standards obtained using the Bruker EDS are also presented in the last four lines in Table 2. It is quite easy to distinguish the different glazing methods and the structures between the essentially quartz-free glaze layer, the interaction layer, and the body, based on the results obtained from laboratory replications, and the microstructural and compositional data from SEM–EDS. The production methods of the faience

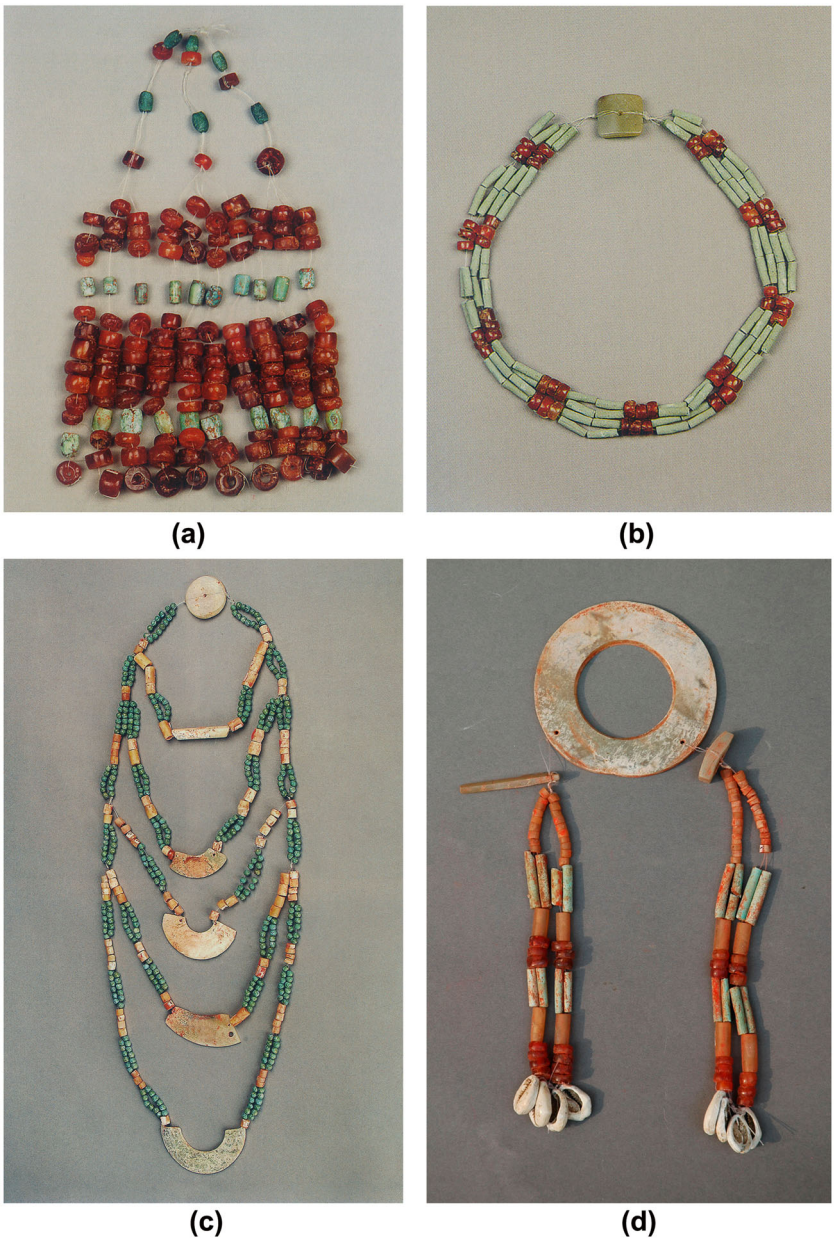


**Fig. 2** Typical photographs of neck ornament and pendant sets, made of faience, carnelian, and jade, unearthed from the Ying State cemetery in Pingdingshan, Henan province (**a**) M231:27, Early Western Zhou Dynasty; (**b**) M201:5, Middle Western Zhou Dynasty; (**c**) M84:128, Middle Western Zhou Dynasty; (**d**) M96:82, Late Western Zhou Dynasty

specimens can be divided into three types based on the cross section physical structures. Sample YJ152-1 belongs to type I with a thick outer blue interaction layer (IAL), and the inner body consists of angular quartz particles in essentially continuous glass matrices (BYD-CGM); PY25-3, PY128-5-2, and PY30, belong to type II with both the IAL and the coarse and loose bodies consisting of angular quartz particles but barely interparticle glasses (IPGs); and PY39-1, PY57-2, PY57-5, PY17, PY21e-1, PY21e-2, and PY21e-3 belong to type III with abundance of IPGs present in the BYD-CGM. The observed microstructures of the beads and tubes vary more or less according to the wall thickness. Due to weathering, the quartz-free glaze layers in most of the faience beads and tubes were absent. The quartz phase of these faience objects can be easily identified by XRD (Dong et al. 2016).

In a study (Vandiver 2008) on the ancient western faience objects, which were formed by the efflorescence glazing method, the objects were characterized by extensive interparticle glasses in the body and variable glaze thickness; in addition, the glaze thickness was the highest on the outer surface and at the rims. The cementation glazing method is characterized by the lack of interparticle glass in the body and by a uniform glaze thickness, whereas the application glazing technique is characterized by the presence of drips and sideway glaze runs, in addition to variable glaze thicknesses. However, some faience objects with thin cross sections, which were

**Table 1** Archeological information of the faience beads unearthed from tombs of the states of Ying and Xu in Pingdingshan, Henan province, China

| Code | Name | No. | Period | Date | Identity of the tomb owner |
|---|---|---|---|---|---|
| PY21e-1 | bead | M231:21e-1 | Early Western Zhou Dynasty | 996–977 BC | Young wife of a duke of Ying (Yinggong) |
| PY21e-2 | bead | M231:21e-2 | Early Western Zhou Dynasty | 996–977 BC | Young wife of a duke of Ying (Yinggong) |
| PY21e-3 | bead | M231:21e-3 | Early Western Zhou Dynasty | 996–977 BC | Young wife of a duke of Ying (Yinggong) |
| PY25-3 | tube | M213:25-3 | Middle Western Zhou Dynasty | 976–922 BC | An aristocracy |
| PY128-5-2 | bead | M84:128-5-2 | Middle Western Zhou Dynasty | 922–900 BC | A marquis named Chen (Yinghou Chen) |
| PY39-1 | bead | M85:39-1 | Middle Western Zhou Dynasty | 937–892 BC | Young wife of a marquis named Chen (Yinghou Chen) |
| PY30 | tube | M107:30 | Late Western Zhou Dynasty | 877–771 BC | An aristocracy |
| PY17 | bead | M269:17 | Late Western Zhou Dynasty | 877–771 BC | A junior aristocracy |
| PY57-2 | tube | M7:57-2 | Early Spring and Autumn period | 771–665 BC | Wife of a senior aristocracy |
| PY57-5 | bead | M7:57-5 | Early Spring and Autumn period | 771–665 BC | Wife of a senior aristocracy |
| YJ152-1 | bead | M4:152-1 | Late Spring and Autumn period | ~ 547 BC | A king of Xu named Ning (Xulinggong) |

produced by the cementation or application glazing methods, are characterized by interparticle glasses within the body and a less well-defined boundary between the interaction layer and the body. The glazing methods used on the faience could be distinguished based on the following three characteristics: the differences in thicknesses between the glaze (GLZ) and interaction layer (IAL); the nature of the boundary between the interaction layer and the body; and the presence or absence of an interparticle glass phase binding the quartz particles in the body (Tite and Bimson 1986; Tite et al. 1983).

In this study, for the type I faience bead, YJ152-1 (with a wall thickness of ~ 2000 μm) has a blue surface layer and a gray light-blue body (Fig. 4b). As shown in Fig. 4a, the thick outer blue layer (typically 150–260 μm in thickness) is not the quartz-free glaze layer but the interaction layer, consisting of angular quartz particles. It was formed on the inner body, which also consists of angular quartz particles in essentially continuous glass matrices. By contrast, the outer layer is much denser than the inner body which contains some scattered pores.

Figure 5 shows the elemental maps of K, Na, and Cu of the specimen YJ152-1, corresponding to the SEM–BSE images of the outer interaction layer (O-IAL) and the inner body consisting of quartz particles in an essentially continuous glass matrix (I-BYD-CGM). Evidently, the interparticle glasses (IPGs) are rich in alkali fluxes containing K and Na, as well as the colorant element, Cu. The presence of thick interaction layer and the interparticle glass in the cores suggests that small amounts of the glazing mixture and an organic binder (such as gum or resin) were mixed with the ground quartz prior to the formation of the faience body, perhaps to produce a more robust body after firing (Shortland and Tite 2005), since it would not have been possible to shape the faience objects in a way with ground quartz and water alone. Thus, some glazing mixture should be applied to the quartz body to facilitate forming the object and to increase its strength both before and after firing, which could result in quartz particles in an essentially continuous glass matrix throughout the body of the object (Vandiver 2008). The characteristics of the well-defined boundary between the interaction layer and the body, and the interparticle glass bonding of the quartz particles both in the interaction layer and in the body, indicate that the efflorescence method was used in the fabrication of the faience bead. Based on the results of quantitative analysis by EDS (Table 2 and Fig. 6), more alkali flux and Cu-containing colorant materials were added into the glazing mixture than those in the quartz sand body. Consequently, a blue interaction layer was adorned on the outer surface, which suggests that the cementation method was probably used after efflorescence. Kiefer and Allibert (1971) successfully replicated a faience object in the laboratory using a combination of efflorescence and cementation methods.

For type II faience tubes (wall thickness: 800–900 μm) and beads (wall thickness: ~ 1000–1300 μm), both the interaction layers (typically 200–250 μm) (Fig. 7a and b) and the bodies consist of abundant angular quartz particles; however, the interparticle glasses (Fig. 7c and d) were barely present in the body. This suggests that either the cementation or the application glazing method was used in the forming process; furthermore, some Cu-containing colorants, perhaps, together with an organic binder, but hardly alkali flux, were applied to the quartz bodies of these faience objects. Even though the glazing mixture was not applied to the quartz body, the interaction layer, associated with cementation or application glazing methods, can still penetrate to depths of up to 1 mm (Vandiver 2008). In contrast to the dense outer interaction layers, the loose inner bodies commonly contain several scatters of pores, which may be due to the volatilization of the organic binder mixed with the bodies during firing.

For type III faience tubes and beads, large amounts of interparticle glasses are present in the bodies, consisting of angular quartz particles embedded in essentially continuous glass matrices (Fig. 8), which indicates that the bodies were

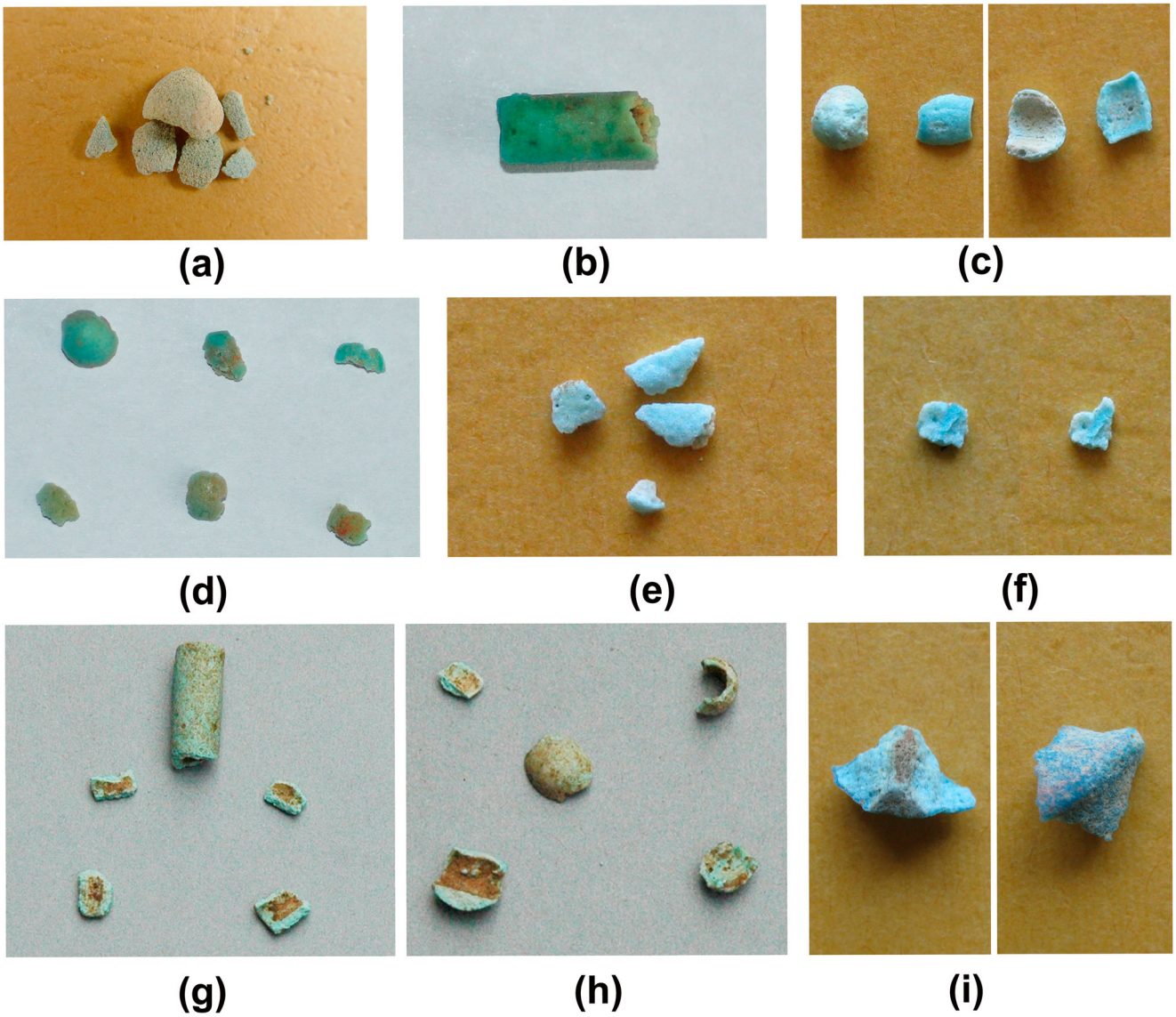


**Fig. 3** Photographs of the analyzed faience fragments (**a**) PY21e; PY25-3; PY128-5, (**c**) PY128-5; (**d**) PY39; (**e**) PY30; (**f**) PY17; (**g**) PY57-2; (**h**) PY57-5; (**i**) YJ152-1

formed by quartz sand mixed with some Cu-containing colorant material and a certain amount of alkali flux as the binder. Since most of the type III faience objects were severely damaged, just the partial cross-sectional images of the bodies could be obtained; but the overall images, from the outer surface to the inner bodies, could not be obtained. However, the remaining glaze layer (merely about 40–80 μm) of the PY39-1 bead was observed on the body with angular quartz particles in essentially continuous glass matrices, whereas the interaction layers are still barely distinguishable (Fig. 8a). The abundant interparticle glass within the bodies consisting of angular quartz particles is an indication that a glazing mixture was applied to their quartz bodies during the forming process and that the cementation glazing method was used. The alkali volatilizes and reacts with the quartz in the faience bodies during firing to form a thin glaze layer, which is then colored by Cu that has also volatilized during firing (Wulff et al. 1968).

However, the thin glaze layer is easily weathered and broken away from the interparticle glass or body. Thus, except for CuO (~6 wt%) and $SiO_2$ (~92 wt%), no $K_2O$ or $Na_2O$ alkali flux was identified in the survived glaze layers of sample PY39-1 and in another fragment of PY128. Weathering often occurred, even in the case of the real ancient glass samples. For example, Liu et al. (2011) have pointed out that the content of $K_2O$ in the glaze layer could be reduced from more than 10 wt% to about 2 wt% in some ancient potash glass. For the small-size faience containing a large amount of quartz and only a small amount of glassy phase, weathering will also lead to the loss of flux in the glassy phase. Especially for the

**Table 2** Chemical composition of the mapping areas in the YJ152-1and PY57-2 samples analyzed by SEM–EDS (COXEM EM-30PLUS) (wt%)

| Sample No. | Phases | $SiO_2$ | $K_2O$ | $Na_2O$ | CuO | Cl | $Al_2O_3$ | CaO | $Fe_2O_3$ | $SO_3$ | MgO | $ZrO_2$ | $P_2O_5$ | $Na_2O/K_2O$ |
|---|---|---|---|---|---|---|---|---|---|---|---|---|---|---|
| YJ152-1-m1 | IAL-BYD-CGM | 91.3 | 3.0 | 1.5 | 2.6 | 0.4 | 0.5 | 0.4 | 0.3 | - | - | - | - | 0.5 |
| YJ152-1-m2 | IAL-BYD-CGM | 90.8 | 2.7 | 1.2 | 2.6 | 0.5 | 0.6 | 0.4 | 0.4 | 0.7 | - | - | - | 0.5 |
| YJ152-1-m3 | IAL-BYD-CGM | 92.1 | 3.3 | 1.0 | 1.3 | 0.7 | 0.6 | 0.5 | 0.5 | - | - | - | - | 0.3 |
| YJ152-1-m4 | IAL-BYD-CGM | 91.1 | 2.8 | 1.3 | 2.8 | 0.4 | 0.6 | 0.4 | 0.3 | 0.5 | - | - | - | 0.5 |
| YJ152-1-m7 | I-BYD-CGM | 91.7 | 2.1 | 1.2 | 2.1 | 0.9 | 0.6 | 0.3 | 0.3 | 0.9 | - | - | - | 0.6 |
| YJ152-1-m8 | O-IAL | 88.2 | 3.9 | 2.0 | 3.7 | 0.4 | 0.8 | 0.5 | 0.3 | -- | 0.3 | - | - | 0.5 |
| YJ152-1-m10 | O-IAL | 88.1 | 4.0 | 2.0 | 3.7 | 0.3 | 1.1 | 0.4 | 0.6 | - | - | - | - | 0.5 |
| YJ152-1-m12 | I-BYD-CGM | 92.8 | 1.8 | 0.8 | 2.1 | 0.5 | 0.4 | - | - | - | - | 1.7 | - | 0.4 |
| PY57-2-m1 | BYD | 95.2 | 0.3 | - | 1.5 | 0.8 | 0.7 | 0.3 | 0.6 | 0.6 | - | - | - | - |
| PY57-2-m2 | BYD-CGM | 94.2 | 1.0 | 0.5 | 1.3 | 0.6 | 0.7 | 0.3 | 1.6 | - | - | - | - | 0.5 |
| PY57-2-m4 | BYD | 92.5 | 0.5 | 0.3 | 1.2 | 0.5 | 0.8 | 0.4 | 0.7 | 0.7 | - | 2.4 | - | 0.7 |
| PY57-2-m6 | BYD-CGM | 93.2 | 1.4 | 0.3 | 0.9 | 0.3 | 0.5 | 0.2 | 2.1 | - | - | - | 1.1 | 0.2 |
| PY57-2-m8 | BYD | 97.2 | 0.2 | - | 1.0 | 0.3 | 0.6 | 0.2 | 0.5 | - | - | - | -- | - |
| PY57-2-m11 | BYD | 90.5 | 0.4 | 0.3 | 0.4 | 1.8 | 0.4 | 0.7 | 0.5 | 0.6 | - | 4.5 | - | 0.9 |
| PY57-2-m12 | BYD | 96.2 | 0.3 | - | 1.2 | 0.4 | 0.8 | 0.2 | - | 1.0 | - | - | - | - |

*BDY*, body; *I*, inner; *O*, outer; *BDY-CGM*, body consisting of quartz particles in an essentially continuous glass matrix

samples in an unsatisfactory condition, the amount of the surviving glassy phases would be less.

Moreover, the glassy phases contain very low-content MgO and CaO in most of the samples, probably due to weathering. This suggests that they would be subject to weathering because the concentration of network stabilizer is too low. In our experimental work, as many glassy phases of these faience objects as possible were analyzed to establish the flux ($Na_2O$ and $K_2O$) content within the IPG phases; however, it is still difficult to detect any ideal flux in some samples. We incline to think that this is caused by weathering, but it needs further research for verification. Since weathering would cause the loss of $Na_2O$ and $K_2O$ even at relatively higher contents without being detected, the low level of MgO and CaO will be also depleted due to their loss in the process of weathering. Besides, the use of mineral alkaline flux is another probable reason for this phenomenon.

In addition, for the majority of the above three types of faience objects, the CuO concentration in the interparticle glass is higher than 3.5 wt%, while the concentration in seven of the samples ranges from 6 to 8 wt%. It appears that the Cu as a colorant material would normally mix into the quartz body to create a blue–green decoration.

## Alkaline flux

The chemical compositions of the interparticle glass and bodies of the faience beads and tubes determined by SEM–EDS are listed in Table 3. Probably due to weathering, the concentration of alkaline flux (i.e., $Na_2O$ and $K_2O$) decreased or disappeared in unpredictable ways, which partly depended on the preservation environment. To obtain the information of the interparticle glass, one to five test points within each sample are sampled for analysis. For the specimens, such as PY21e-1, PY21e-2, PY21e-3, Y39-1, PY30, PY57-2, and YJ152-1, in which the alkali flux of the interparticle glass is distinctly higher than in the other samples, the average values of their total alkali content ($Na_2O + K_2O$) vary from 13.6 to 20.3 wt%. In contrast, the total alkali content of the interparticle glass in PY17 is just 5.6 wt%, whereas for PY25-3, PY128-5-2, and PY17, the total alkali contents are less than 0.5 wt%. Try as we might, we could not identify the alkaline flux in the interparticle glass of sample PY57-5. The low total alkali contents (below 6 wt%) of these samples were probably due to weathering, glazing methods, preservation environment, or for some other reasons, which needs to be further investigated.

Generally, the western faience objects are characterized by soda-rich alkali fluxes, including soda-rich plant ashes and natron, the result of natural evaporation; soda is the dominant alkali (Vandiver 2008). The faience objects of different chemical types (i.e., soda-rich, mixed-alkali, and potash-rich faience objects) can be identified based on their total alkali and soda to potash ratio in the glaze and interparticle glass. The mixed-alkali vitreous materials typically contain between ca. 4–9 wt% $Na_2O$, ca. 6–12 wt% $K_2O$, and ca. 0.5–1.0 wt% MgO. They are normally referred to as low-magnesium and high-potassium glasses (LMHK) (Henderson 1988; Henderson et al. 2015; Tite and Shortland 2008). Vandiver et al. (2008) addressed the criteria for soda-rich and mixed-alkali categories. Based on which, Lin et al. (2019) preliminarily discussed the criterion for the potash-rich category, taking the mixed-alkali and potash-rich faience objects,

**Table 3** Chemical compositions of the faience objects investigated in this study, analyzed by SEM–EDS (wt%)

| Code | IPG | $Na_2O$ | $K_2O$ | CuO | $SiO_2$ | Cl | $Al_2O_3$ | CaO | $Fe_2O_3$ | $SO_3$ | MgO | $ZrO_2$ | $TiO_2$ | MnO | $Na_2O/K_2O$ | Alkali type | $Na_2O+K_2O$ | $K_2O/Na_2O$ | $Na_2O/(Na_2O+K_2O)$ | $K_2O/(Na_2O+K_2O)$ |
|---|---|---|---|---|---|---|---|---|---|---|---|---|---|---|---|---|---|---|---|---|
| PY21e-1 | IPG1 | 15.8 | 2.9 | 5.3 | 70.3 | 0.9 | 3.4 | - | 1.3 | - | - | - | - | - | 5.45 | Soda-rich | 18.7 | 0.18 | 0.845 | 0.155 |
| PY21e-1 | IPG2 | 18.2 | 3.6 | 7.5 | 64.9 | 1.1 | 2.8 | 0.7 | 1.2 | - | - | - | - | - | 5.06 | Soda-rich | 21.8 | 0.20 | 0.835 | 0.165 |
| PY21e-1-IPG-STD | | 1.2 | 0.4 | 1.1 | 2.7 | 0.1 | 0.3 | 0.0 | 0.1 | - | - | - | - | - | 0.20 | | 1.6 | 0.29 | 0.774 | 0.226 |
| PY21e-1-IPG-Average | | 17.0 | 3.3 | 6.4 | 67.6 | 1.0 | 3.1 | 0.7 | 1.3 | - | - | - | - | - | 5.3 | Soda-rich | 20.3 | 0.19 | 0.840 | 0.160 |
| PY21e-2 | IPG1 | 10.5 | 4.0 | 6.8 | 69.9 | 1.3 | 3.5 | - | 2.1 | - | - | | 1.8 | - | 2.63 | Soda-rich | 14.5 | 0.38 | 0.724 | 0.276 |
| PY21e-2 | IPG2 | 16.5 | 3.7 | 5.3 | 67.7 | 0.9 | 4.2 | - | 1.7 | - | - | - | - | - | 4.46 | Soda-rich | 20.2 | 0.22 | 0.817 | 0.183 |
| PY21e-2 | IPG3 | 16.2 | 3.4 | 6.0 | 68.4 | 1.1 | 3.3 | - | 1.5 | - | - | - | - | - | 4.76 | Soda-rich | 19.6 | 0.21 | 0.827 | 0.173 |
| PY21e-2-IPG-STD | | 2.8 | 0.2 | 0.6 | 0.9 | 0.2 | 0.4 | - | 0.2 | - | - | - | | - | 0.94 | | 2.6 | 0.08 | 0.046 | 0.046 |
| PY21e-2-IPG-Average | | 14.4 | 3.7 | 6.0 | 68.7 | 1.1 | 3.7 | - | 1.8 | - | - | - | 1.8 | - | 3.95 | Soda-rich | 18.1 | 0.27 | 0.789 | 0.211 |
| PY21e-3 | IPG1 | 4.5 | 11.8 | 6.5 | 72.9 | - | 2.7 | 1.0 | - | - | 0.5 | - | - | - | 0.38 | Potash-rich | 16.3 | 2.62 | 0.276 | 0.724 |
| PY21e-3 | IPG2 | 5.5 | 12.5 | 6.2 | 70.8 | - | 1.4 | 3.1 | - | - | 0.5 | - | - | - | 0.44 | Potash-rich | 18.0 | 2.27 | 0.306 | 0.694 |
| PY21e-3 | IPG3 | 4.6 | 14.3 | 8.7 | 68.8 | - | 1.3 | 2.3 | - | - | - | - | - | - | 0.32 | Potash-rich | 18.9 | 3.11 | 0.243 | 0.757 |
| PY21e-3-IPG-STD | | 0.4 | 1.1 | 1.1 | 1.7 | - | 0.6 | 0.9 | - | - | 0.0 | - | | - | 0.05 | | 1.1 | 0.34 | 0.025 | 0.025 |
| PY21e-3-IPG-Average | | 4.9 | 12.9 | 7.1 | 70.8 | - | 1.8 | 2.1 | - | - | 0.5 | - | | - | 0.38 | Potash-rich | 17.7 | 2.67 | 0.275 | 0.725 |
| PY25-3 | IPG1 | 0.1 | 0.2 | 6.8 | 90.4 | 0.9 | 1.1 | 0.4 | - | - | 0.1 | - | - | - | 0.50 | | 0.3 | 2.00 | 0.333 | 0.667 |
| PY25-3 | IPG2 | 0.1 | - | 6.9 | 91.2 | 0.9 | 0.8 | 0.1 | - | - | 0.1 | - | - | - | - | | 0.1 | 0.00 | 1.000 | 0.000 |
| PY25-3-IPG-STD | | 0.0 | 0.1 | 0.1 | 0.4 | 0.0 | 0.2 | 0.2 | - | - | 0.0 | - | - | - | - | | 0.1 | 1.00 | 0.333 | 0.333 |
| PY25-3-IPG-Average | | 0.1 | 0.1 | 6.9 | 90.8 | 0.9 | 1.0 | 0.3 | - | - | 0.1 | - | - | - | 0.50 | | 0.2 | 1.00 | 0.667 | 0.333 |
| PY25-3 | Particle 3 | 1.0 | 0.5 | 4.0 | 7.4 | 0.2 | 24.9 | 7.3 | 46.2 | - | 4.6 | - | 3.8 | 0.2 | 2.00 | | 1.5 | 0.50 | 0.667 | 0.333 |
| PY128-5-2 | IPG1 | - | - | 9.3 | 88.2 | 2.0 | 0.4 | - | - | - | - | - | - | - | - | | - | - | - | - |
| PY128-5-2 | IPG2 | - | - | 6.9 | 90.9 | 1.5 | 0.0 | 0.4 | - | - | 0.3 | - | - | - | - | | - | - | - | - |
| PY128-5-2-IPG-STD | | - | - | 1.2 | 1.4 | 0.3 | 0.2 | 0.0 | - | - | 0.0 | - | - | - | - | | - | - | - | - |
| PY128-5-2-IPG-Average | | - | - | 8.1 | 89.6 | 1.8 | 0.2 | 0.4 | - | - | 0.3 | - | - | - | - | | - | - | - | - |
| PY39-1 | IPG1 | 3.6 | 13.3 | 3.4 | 75.4 | 0.2 | 1.1 | 2.5 | - | - | 0.4 | - | - | - | 0.27 | Potash-rich | 16.9 | 3.69 | 0.213 | 0.787 |
| PY39-1 | IPG2 | 3.0 | 15.5 | 3.3 | 73.7 | 0.1 | 0.8 | 2.1 | 0.2 | - | 1.4 | - | - | - | 0.19 | Potash-rich | 18.5 | 5.17 | 0.162 | 0.838 |
| PY39-1-IPG-STD | | 0.3 | 1.1 | 0.1 | 0.9 | 0.1 | 0.2 | 0.2 | 0.0 | - | 0.5 | - | - | - | 0.04 | | 0.8 | 0.74 | 0.025 | 0.025 |
| PY39-1-IPG-Average | | 3.3 | 14.4 | 3.4 | 74.6 | 0.2 | 1.0 | 2.3 | 0.2 | - | 0.9 | - | - | - | 0.23 | Potash-rich | 17.7 | 4.43 | 0.188 | 0.812 |
| PY30 | IPG1 | 0.8 | 19.9 | 1.4 | 58.6 | 0.3 | 0.2 | 0.1 | 18.7 | - | - | - | - | - | 0.04 | Potash-rich | 20.7 | 24.88 | 0.039 | 0.961 |
| PY30 | IPG2 | 1.0 | 15.5 | 0.9 | 70.9 | 0.1 | 0.4 | - | 11.2 | - | - | - | - | - | 0.06 | Potash-rich | 16.5 | 15.50 | 0.061 | 0.939 |
| PY30-IPG-STD | | 0.1 | 2.2 | 0.3 | 6.2 | 0.1 | 0.1 | 0.0 | 3.8 | - | - | - | - | - | 0.01 | | 2.1 | 4.70 | 0.011 | 0.011 |
| PY30-IPG-Average | | 0.9 | 17.7 | 1.2 | 64.8 | 0.2 | 0.3 | 0.1 | 15.0 | - | - | - | - | - | 0.05 | Potash-rich | 18.6 | 20.19 | 0.050 | 0.950 |

**Table 3** (continued)

| Code | IPG | $Na_2O$ | $K_2O$ | CuO | $SiO_2$ | Cl | $Al_2O_3$ | CaO | $Fe_2O_3$ | $SO_3$ | MgO | $ZrO_2$ | $TiO_2$ | MnO | $Na_2O/K_2O$ | Alkali type | $Na_2O+K_2O$ | $K_2O/Na_2O$ | $Na_2O/(Na_2O+K_2O)$ | $K_2O/(Na_2O+K_2O)$ |
|---|---|---|---|---|---|---|---|---|---|---|---|---|---|---|---|---|---|---|---|---|
| PY17 | IPG (BO-Y) | 2.1 | 3.5 | 3.9 | 72.6 | 5.2 | | 5.1 | - | 6.4 | 1.0 | - | - | - | 0.60 | Very likely mixed--alkali | 5.6 | 1.67 | 0.375 | 0.625 |
| PY57-2-p1 | IPG1 | 2.1 | 13.0 | 1.4 | 70.8 | 0.3 | 0.7 | 0.0 | 11.7 | 0.0 | - | - | - | - | 0.16 | Potash-rich | 15.1 | 6.07 | 0.142 | 0.858 |
| YJ152-1-p9 | IPG9 | 5.5 | 9.0 | 7.3 | 73.6 | 0.8 | 1.7 | 1.1 | 0.6 | 0.0 | 0.6 | 0.0 | - | - | 0.61 | Mixed-alkali | 14.4 | 1.64 | 0.379 | 0.621 |
| YJ152-1-p10 | IPG10 | 4.0 | 10.9 | 9.1 | 70.7 | 0.7 | 2.2 | 1.3 | 0.6 | 0.0 | 0.5 | 0.0 | - | - | 0.37 | / | 14.9 | 2.71 | 0.270 | 0.730 |
| YJ152-1-p11 | IPG11 | 4.9 | 4.8 | 2.8 | 20.6 | 0.4 | 34.0 | 0.0 | 32.5 | 0.0 | 0.0 | 0.0 | - | - | 1.04 | Mixed-alkali | 9.7 | 0.97 | 0.509 | 0.491 |
| YJ152-1-p12 | IPG12 | 5.1 | 9.9 | 8.9 | 71.0 | 0.7 | 1.9 | 1.0 | 0.7 | 0.0 | 0.8 | 0.0 | - | - | 0.52 | Mixed-alkali | 15.0 | 1.93 | 0.341 | 0.659 |
| YJ152-1-p13 | IPG13 | 1.9 | 2.7 | 2.7 | 91.5 | 0.0 | 0.8 | 0.0 | 0.0 | 0.0 | 0.3 | 0.0 | - | - | 0.71 | Very likely mixed--alkali | 4.6 | 1.42 | 0.414 | 0.586 |
| YJ152-1-p16 | IPG16 | 5.1 | 8.8 | 9.2 | 72.1 | 0.5 | 2.1 | 1.0 | 0.5 | 0.0 | 0.0 | 0.7 | - | - | 0.57 | Mixed-alkali | 13.9 | 1.74 | 0.365 | 0.635 |
| YJ152-1-IPG-STD | | 1.2 | 2.9 | 2.8 | 21.8 | 0.3 | 12.0 | 0.5 | 11.9 | 0.0 | 0.3 | 0.3 | - | - | 0.21 | | 3.8 | 0.53 | 0.073 | 0.073 |
| YJ152-1-IPG-Average | | 4.4 | 7.7 | 6.7 | 66.6 | 0.5 | 7.1 | 0.7 | 5.8 | 0.0 | 0.4 | 0.1 | - | - | 0.64 | Mixed-alkali | 12.1 | 1.73 | 0.379 | 0.621 |
| Glass standards | | $Na_2O$ | $K_2O$ | CuO | $SiO_2$ | Cl | $Al_2O_3$ | CaO | $Fe_2O_3$ | $SO_3$ | MgO | $ZrO_2$ | $TiO_2$ | MnO | BaO | $Sb_2O_5$ | PbO | $P_2O_5$ | CoO | Sum |
| Corning glass B (PB ZAF) | | 20.1 | 1.4 | 2.8 | 57.8 | | 4.4 | 8.8 | 0.5 | | 1.1 | | 0.1 | 0.3 | - | 0.5 | 0.3 | 0.9 | | 99 |
| Reference content | | 17.00 | 1.00 | 2.66 | 61.55 | | 4.36 | 8.56 | 0.34 | | 1.03 | | 0.089 | 0.25 | 0.12 | 0.46 | 0.61 | 0.82 | 0.046 | 99 |
| Corning glass C(PB ZAF) | | 0.9 | 2.8 | 1.4 | 28.3 | | 0.7 | 5.9 | 0.4 | | 2.8 | | 0.6 | 0.8 | 12.9 | - | 40.1 | - | - | 98 |
| Reference content | | 1.07 | 2.84 | 1.13 | 34.87 | | 0.87 | 5.07 | 0.34 | | 2.76 | | 0.79 | 0.82 | 11.4 | 0.03 | 36.7 | 0.14 | 0.18 | 99 |
| Corning glass D (PB ZAF) | | 1.2 | 15.0 | 0.3 | 47.2 | | 4.9 | 21.7 | 0.7 | | 3.5 | | 0.6 | 0.8 | - | - | - | 4.0 | - | 100 |
| Reference content | | 1.2 | 11.3 | 0.38 | 55.24 | | 5.30 | 14.8 | 0.52 | | 3.94 | | 0.38 | 0.55 | 0.51 | 0.97 | 0.48 | 3.93 | 0.023 | 100 |

YJ152-1 and PY57-2 analyzed by Oxford X-act compact 1414 EDS; the others by Bruker Nano Gmbh 610 M EDS

*BYD*, body; *IPG*, interparticle glass; *STD*, standard deviation

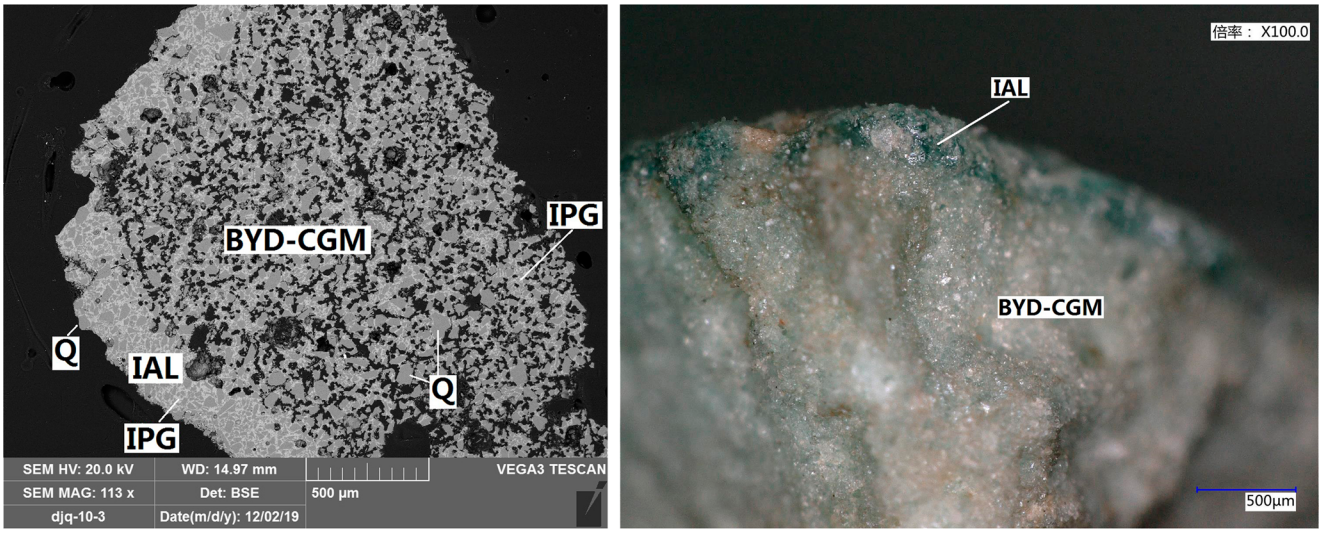


**Fig. 4** Microscopic morphology images of YJ152-1 (**a**) SEM–BSE image by COXEM EM-30PLUS SEM; (**b**) Micro-photograph by VHX-5000 Digital Microscopy. IAL, interaction layer; BYD-CMG, body consisting of quartz particles in an essentially continuous glass matrix; IPG, interparticle glass; Q, quartz particle

dated to the Bronze Age, unearthed in Qinghai and Xinjiang provinces, as examples. Nevertheless, the data selection process is not ideal. The faience objects with a soda to potash ratio significantly above 1.5 in the glaze are classified as soda-rich, while mixed-alkali faience objects typically have a ratio of 0.5–1.5. The total alkali levels are typically above 6–7 wt%; however, for soda-rich faience, the minimum levels of total alkali should be above 4 wt%. The Na/K ratio below circa 0.4 on average with a total alkali content of at least 7 wt% was suggested as the criterion for potash-rich faience by Lin et al. (2019).

According to the above criteria and the average values of the interparticle glass listed in Table 3, the PY21e-1 and PY21e-2 samples dated to the early Western Zhou Dynasty (1046–977 BC) are considered soda-rich types with high contents of $Na_2O$ (14.4 and 17.0 wt%, respectively) and low contents of $K_2O$ (around 3.5 wt%), and the $Na_2O/K_2O$ ratios

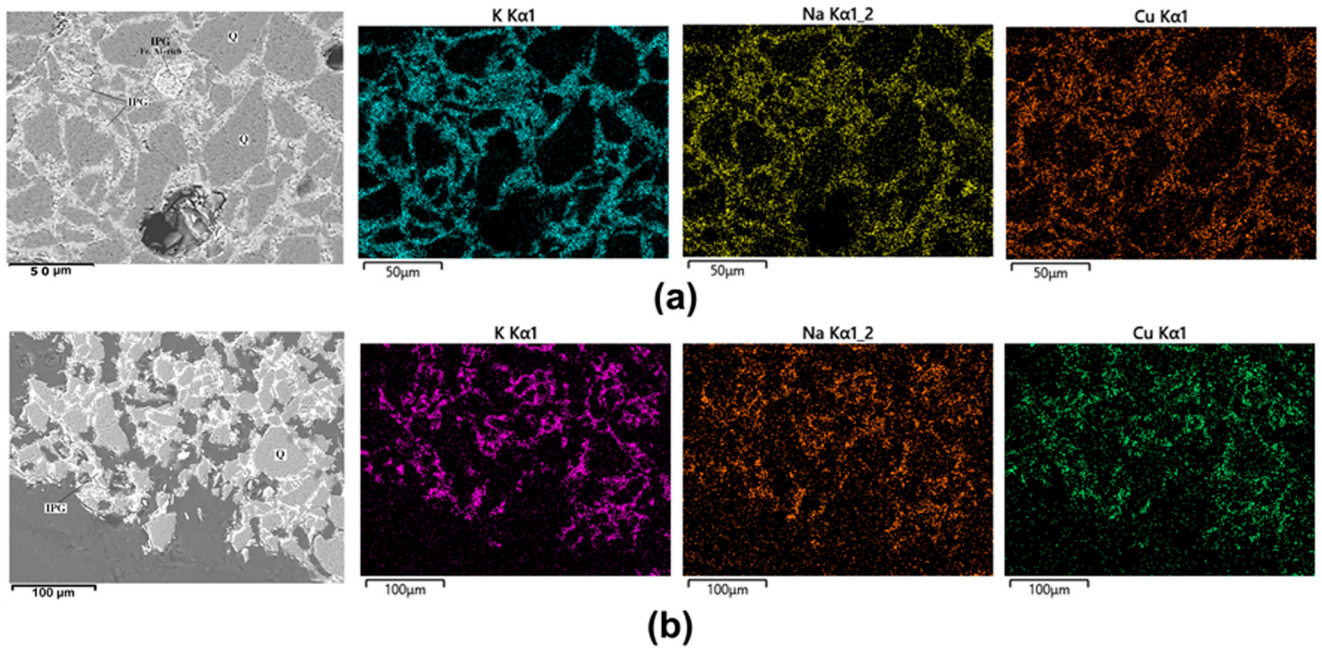


**Fig. 5** SEM–BSE images and EDS mapping of K, Na, and Cu elements of YJ152-1. The light shade corresponds to a high concentration. (**a**) YJ152-1-m10, outer interaction layer; (**b**) YJ152-1-m7, inner body consisting of quartz particles in an essentially continuous glass matrix; IPG, interparticle glass; Q, quartz particle

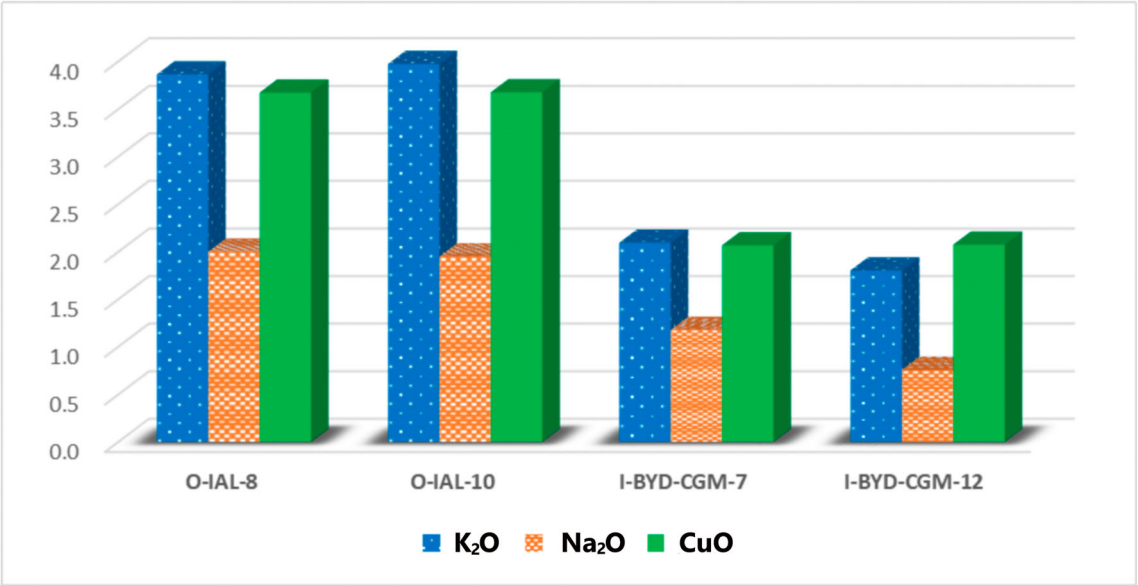


**Fig. 6** Bar chart of $K_2O$, $Na_2O$, and CuO contents in the surface layer and interior of sample YJ152-1. O-IAL, outer interaction layer; I-BYD-CMG, inner body consisting of quartz particles in an essentially continuous glass matrix

are 3.95 and 5.25; the PY21e-3, PY39-1, PY30, and PY57-2 samples dating from the early Western Zhou Dynasty to the early Spring and Autumn period (from about the middle eleventh to middle fifth century BC) belong to the potash-rich group, with 13.0–17.7 wt% of $K_2O$, 2.1–4.9 wt% of $Na_2O$, and a $Na_2O/K_2O$ ratio below 0.5. Six different regions in the IPG phase of sample YJ152-1 were analyzed by SEM–EDS. Among them, four regions contain 4.8–9.9 wt% $K_2O$ and 4.9–5.5 wt% $Na_2O$, with the $Na_2O/K_2O$ ratio ranging from 0.52 to 1.04. Meanwhile, the magnesia, lime, and phosphorus contents are very low (< 1 wt% MgO, < 1.5 wt% CaO, and < 0.1 wt% $P_2O_5$). It indicates that this sample could be termed LMHP mixed-alkali faience. However, there are also two anomalous regions. The total alkali ($K_2O$ + $Na_2O$) content of one of the anomalous region is only 4.6 wt% (< 7 wt%), while in the other region, the concentrations of the potassium oxide and sodium oxide are 10.9 and 4.0 wt%, respectively; thus, the $Na_2O/K_2O$ ratio is below 0.5. The inconsistency in the chemical analysis of micro areas do exist, and this inconsistency may be due to several factors such as weathering and the heterogeneity of raw materials. In addition, although the total alkali of sample PY17 is also slightly lower than 7 wt% (only 5.6 wt%), the $Na_2O/K_2O$ ratio is 0.6, which is similar to that of the mixed-alkali type. But the CaO content (5.1 wt%) is higher than the others.

By combining the previous reports (Brill et al. 1989; Dong et al. 2016; Gu 2015; Lei and Xia 2015; Li et al. 2009; Lin et al. 2019; Liu et al. 2017; Liu et al. 2019; Wang 2019; Wang et al. 2020), the faience objects unearthed in China, dated from the Western Zhou Dynasty (1046–771 BC) to the Spring and Autumn period (770–476 BC), are mainly distributed in the Western and Central China, including Xinjiang, Qinghai, Gansu, Shaanxi, Shanxi, and Henan provinces (Fig. 9). The earliest faience beads are unearthed from Adunqiaolu, an early Bronze Age site (1689–1528 BC), in the western Xinjiang province. Many faience objects were found in the sites of the Zhou Dynasty (1046–476 BC) along the Yellow River Basin, while the faience objects unearthed in the Yangtze River Basin, including Hubei, Sichuan, and Jiangsu provinces, are slightly younger than those of the above regions, dating from the middle Western Zhou Dynasty to the Warring States period (from around the middle of the tenth century to the third century BC) (Gu 2015; Lin and Rehren 2017; Wang 2019; Zhao et al. 2011).

In the present study, the $Na_2O/K_2O$ ratios of the specimens are compared with the published data (Brill et al. 1989; Lei and Xia 2015; Liu et al. 2019; Lin et al. 2019; Wang et al. 2020) to study the provenances of the faience objects unearthed in Pingdingshan, Henan province, and the possible distribution pattern and exchange strategy of the faience objects between Pingdingshan and the surrounding regions. Based on the aforementioned criteria, the alkaline flux types of these faience objects are shown in Fig. 10a.

The faience objects with a $Na_2O/K_2O$ ratio less than 0.5 are classified as potash-rich. Since the faience objects of the potash-rich type are close to those of the mixed-alkali type with a $Na_2O/K_2O$ ratio less than 1, we attempted to use the $Na_2O/(Na_2O + K_2O)$ ratio to distinguish them (Fig. 10b). It appears that the faience objects with the ratios above 0.6, between 0.3 and 0.6, and below 0.3 could be classified as soda-rich, mixed-alkali, and potash-rich ones, respectively. The soda-rich and mixed-alkali faience objects mainly originate from Gansu and Xinjiang provinces, respectively. For the mixed-alkali type, the faience objects unearthed from the

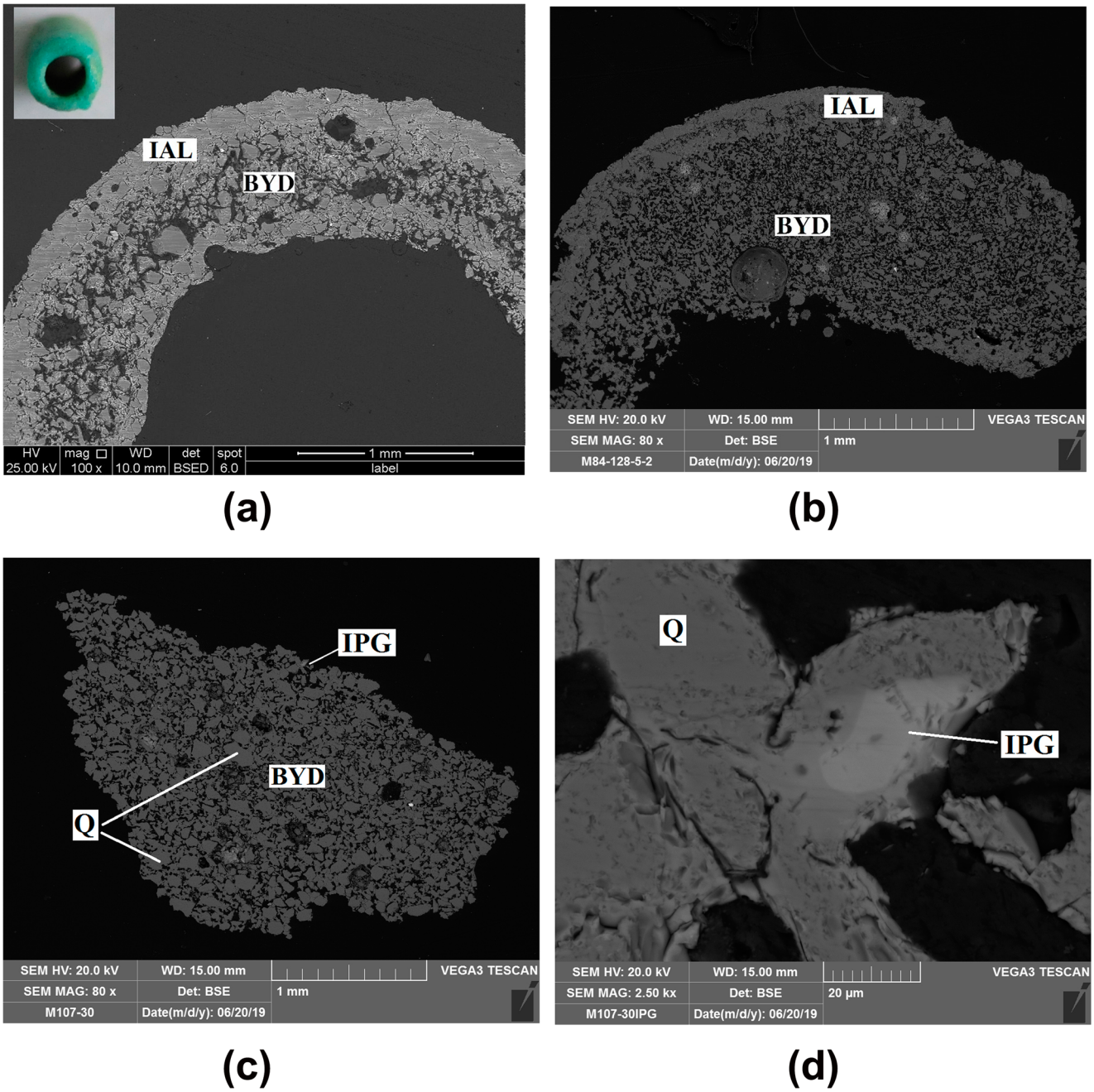


**Fig. 7** BSE image of samples (**a**) PY25-3, (**b**) PY128-5-2, (**c**) PY30, (**d**) PY57-2, and (**e**) PY39-1

Tianshanbeilu site have lower levels of total alkali than those from the Adunqiaolu site, Xinjiang province. The lower levels of total alkali for samples found in Tianshanbeilu site range from 7.10 to 15.72 wt%, while the higher levels of total alkali for samples found in Adunqiaolu site range from 13.32 to 17.24 wt%. In addition, all the faience objects from Central China and the Qinghai province have a higher amount of potash than soda, while the ratios of soda to potash in those from Xinjiang vary from 0.5 to 1.

Figure 11 shows the alkaline flux types along with the period of the faience objects unearthed in Central China of different periods from the Western Zhou to the Spring and Autumn Dynasty (1046–476 BC). There are only three soda-rich and one potash-rich faience beads of the early Western Zhou Dynasty. The number of the faience objects of the two flux types increased significantly in the middle Western Zhou Dynasty (976–878 BC), and the potash-rich faience objects were prevalent in those days. Thereafter, the number of faience objects decreased gradually; furthermore, the soda-rich faience disappeared and was replaced by mixed-alkali faience objects dated from the late Western Zhou Dynasty (877–771 BC) to the late Spring and Autumn period

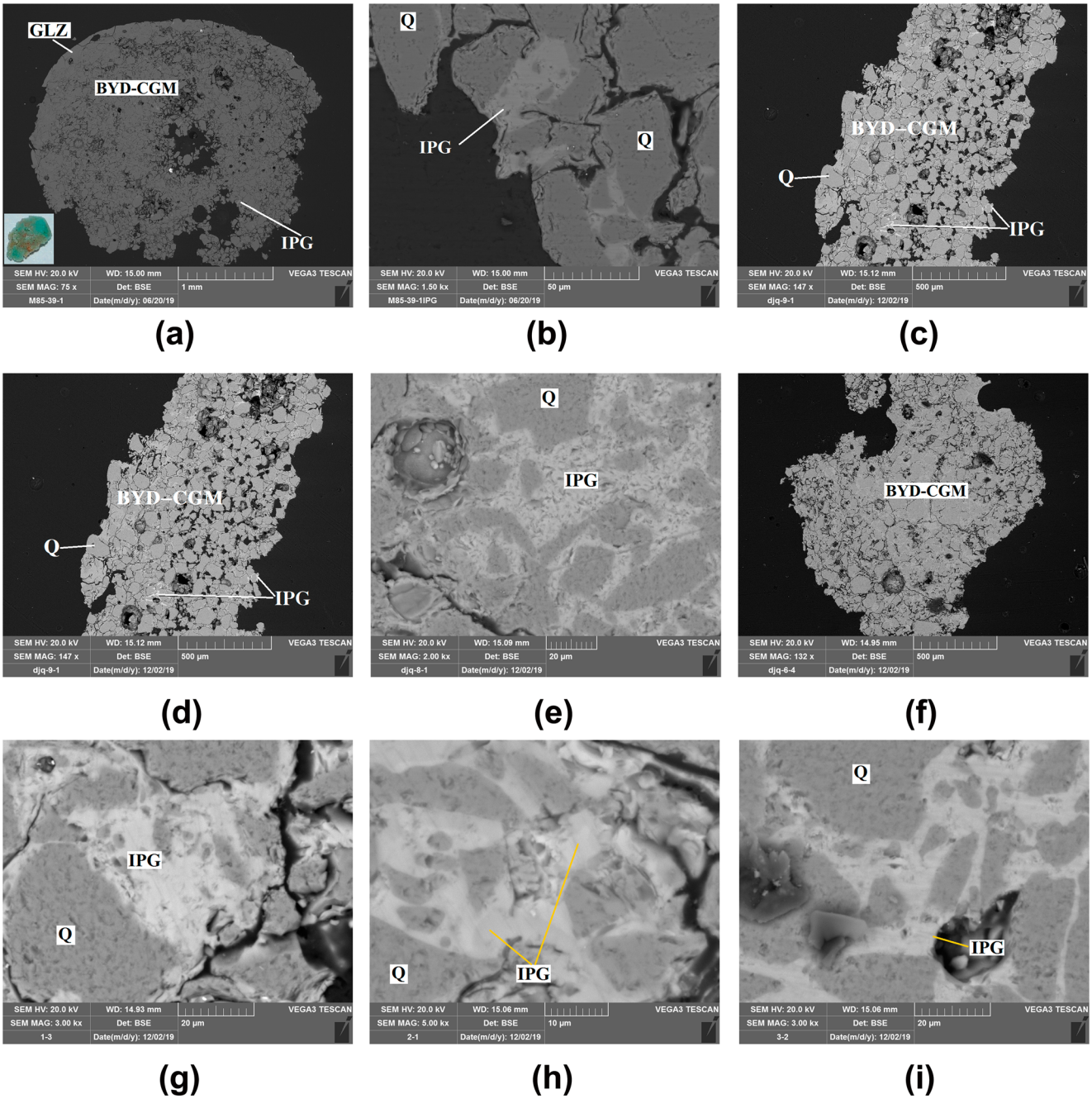


**Fig. 8** BSE image of type III faience objects: (**a**) PY39-1, (**b**) PY39-1, (**c**) PY57-2, (**d**) PY57-2, (**e**) PY575, (**f**) PY17, (**g**) PY21e-1, (**h**) PY21e-2, and (**i**) PY21e-3

(around 547 BC). The transition of the alkaline flux of the faience objects from Central China is an indication of the variation in the provenances.

## Provenances

Based on the results of this study and the previous studies, the faience objects unearthed in Pingdingshan, Henan province, have more than one provenance. Firstly, it can be concluded that the soda-rich faience objects of the early Western Zhou Dynasty were imported from somewhere along the route from Egypt to Central China, the same as the ones from Shaanxi and Shanxi provinces (Lei and Xia 2015).

The lead isotope analysis results of the potash-rich faience bead (5895, Pb-3400), unearthed in Fengxi, Shanxi province with 15.00 wt% $K_2O$, 2.85 wt% $Na_2O$, and 8.16 wt% CuO in the interstitial glass phase (Brill et al. 1989), showed that it belonged in the lowest lead isotope ratio group ($^{208}Pb/^{206}Pb$: 1.9621, $^{207}Pb/^{206}$: 0.79111, and $^{204}Pb/^{206}$ Pb: 0.04938) (Brill and Martin 1991; Brill et al. 1991) that was regarded as a

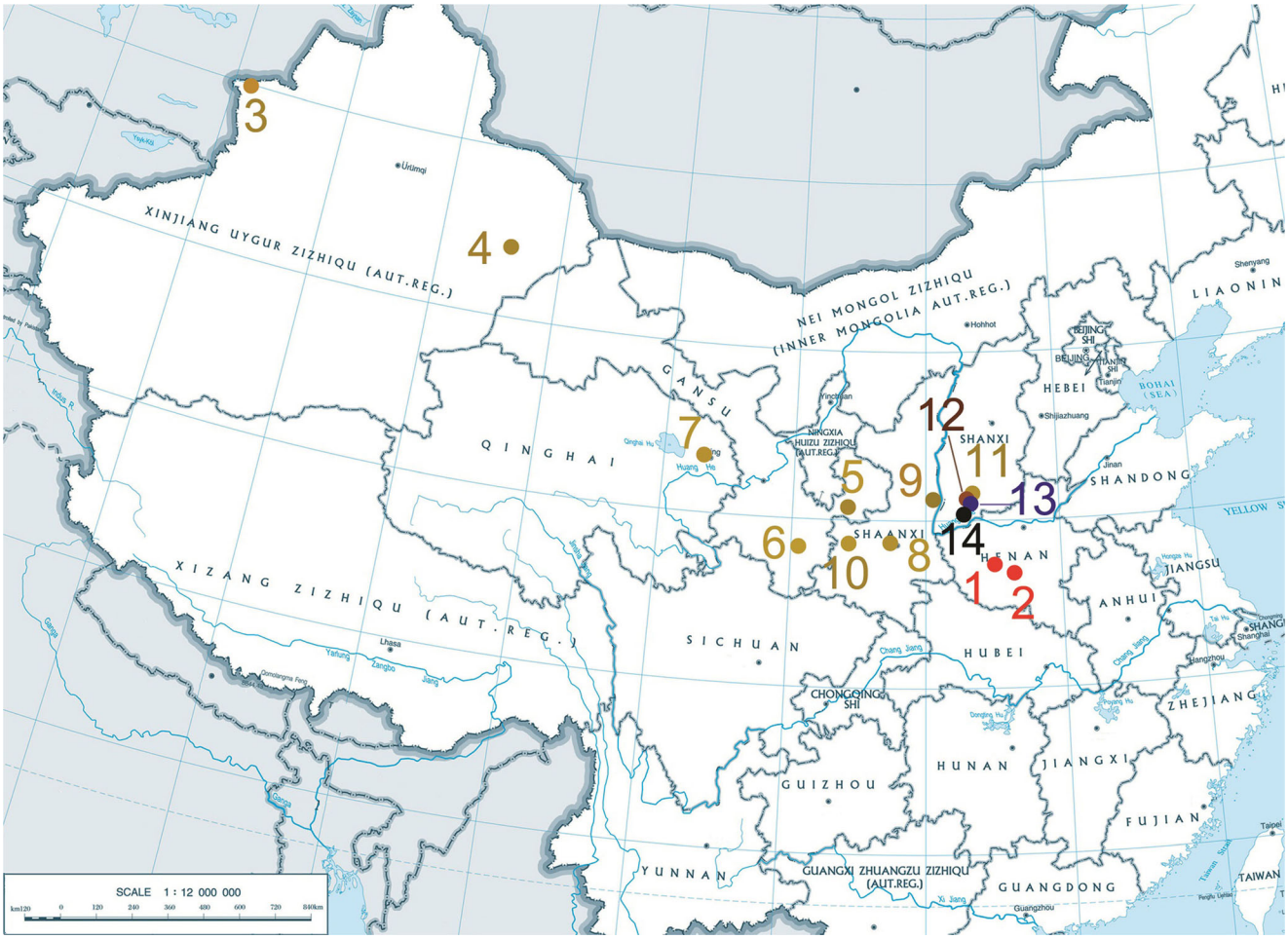


**Fig. 9** Typical sites of faience objects in China (around ca. 16–ca. 5 BC). 1. Ying State Cemetery, Pingdingshan; 2. Xu State Cemetery, Jiuxian, Ye; 3. Adunqiaolu Cemetery, Wenquan; 4. Tianshanbeilu, Hami; 5. Yujiawan, Chongxin; 6. Dapuzishan, Li; 7. Shangsunjiazhai, Datong; 8. Fengxi, Xi'an; 9. Rui State Cemetery, Liangdaicun, Weinan; 10. Zhuyuangou, Baoji; 11. Dahekou, Yicheng; 12. Jin State Cemetery, Tianma-Qucun; 13. Jin State Cemetery, Yangshe, Quwo; 14. Peng State Cemetery, Hengshui, Jiang

typical Chinese isotopic type, which suggests that the faience bead was made in ancient China. This is a reliable evidence of the Chinese native origin of the potash-rich faience.

Recently, Lin et al. (2019) assumed that the Kayue people in the Qinghai province were the first to use high potash glaze recipes and that they began producing faience objects with a high potash content during the second half of the 2nd millennium BC, prior to the Western Zhou Dynasty (1046–771 BC) in Central China, i.e., Shaanxi and Shanxi provinces. They concluded that the Zhou people learned these techniques from their pastoralist neighbors from the West, i.e., the Kayue people, and perfected it themselves. However, Yang (2020) have demonstrated that there is insufficient evidence to support the claim that high potash faience was introduced into China before the Western Zhou Dynasty.

As shown in Figs. 9 and 10, the potash-rich faience objects are widely found in the Yellow River Basin, concentrated in Central China, including Fengxi and Zhuyuangou in Shaanxi, Tianma-Qucun, Yangshe, Hengshui, and Dakekou in Shanxi, Pingdingshan in Henan, and its environs (i.e., Dapuzishan and Yujiawan in Gansu). In contrast, there are just four faience beads from one site (Shangsunjiazhai) in Qinghai province. In addition, the date of the Kayue culture tombs at the Shangsunjiazhai site, from which the analyzed faience beads were obtained, has been a source of controversy (Zhang 2003; Zhang 2009). Yang (2020) argued that there is no solid evidence to support the hypothesis that the potash-rich faience beads unearthed from Shangsunjiazhai predate the Western Zhou Dynasty (1046–771 BC), i.e., probably younger than 900 BC. Therefore, it cannot be concluded that the Zhou people learned the techniques for producing high potash faience objects from the Kayue people.

Regardless of the prevalent time or distribution regions, it appears that the craftsmen of the Western Zhou Dynasty in Central China are more likely to have produced potash-rich faience than the nomads of the Kayue culture in Shangsunjiazhai, Qinghai. Thus, we assume that the analyzed

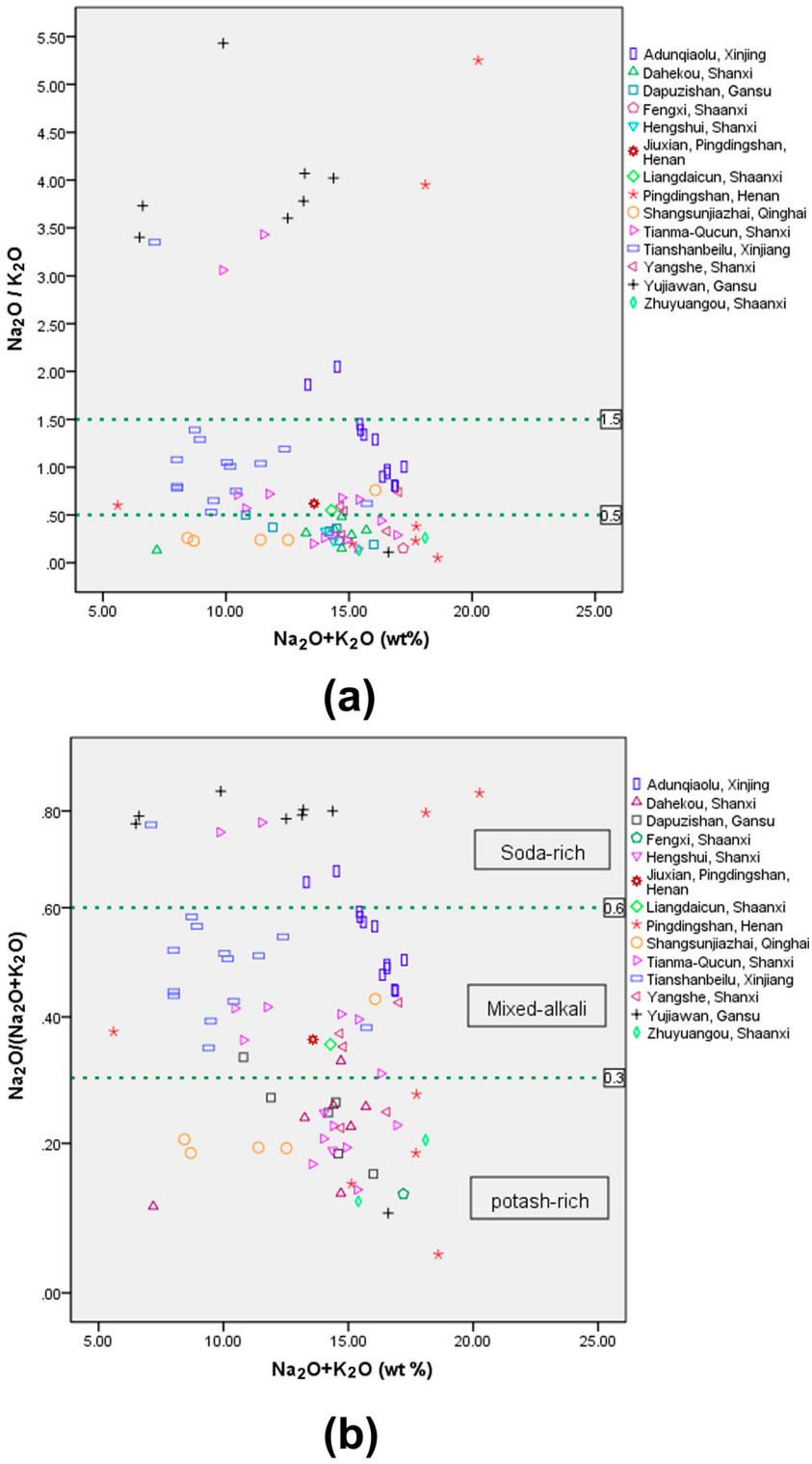


**Fig. 10** Total alkali contents vs (**a**) $Na_2O/K_2O$ ratio, and (**b**) $Na_2O/(Na_2O + K_2O)$ ratio of IPG in the three alkali types of faience objects unearthed in China

potash-rich faience objects from Pingdingshan were produced locally or in the surrounding regions within the Zhou realm.

A high potash content is a typical feature of Chinese faience objects. Therefore, a soda/potash ratio of less than 1 was once regarded as the main criterion for distinguishing Chinese native faience objects from those of the West (Liu et al. 2017; Lei and Xia 2015; Gu et al. 2014; Fu and Gan 2006). In fact, the potash-dominated faience objects (i.e., $K_2O > Na_2O$) include the aforementioned partial mixed-alkali flux objects, in which the potash content is comparable to, or greater than, the soda content.

Wang et al. (2019) reported that the earliest mixed-alkali faience objects, unearthed from the Adunqiaolu site, Xinjiang,

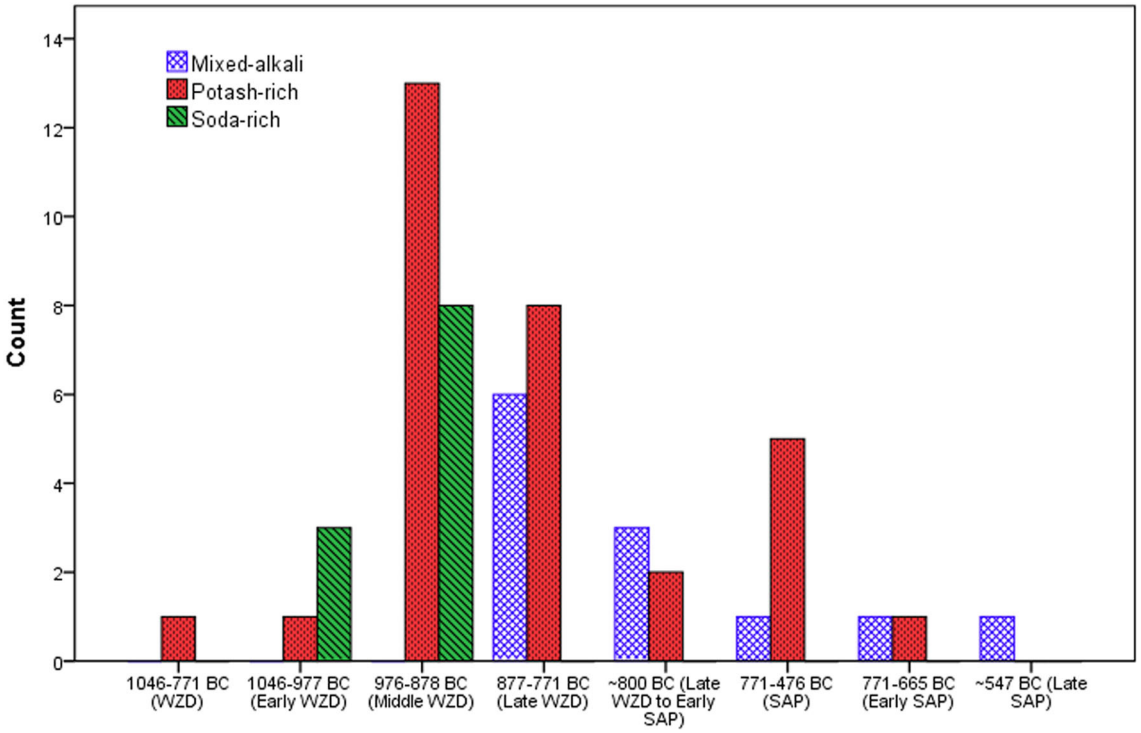


**Fig. 11** Comparison in the number of faience objects of different alkaline flux types found in Central China during different periods of the Zhou Dynasty (1046–476 BC) (WZD, Western Zhou Dynasty; SAP, Spring and Autumn period)

have a strong correlation with those from the Eurasian Steppe and Europe. Liu et al. (2017) and Yang (2020) suggested that there was a possible route for the transfer of faience production technologies from Western Asia through Xinjiang to Central China about 3000 years ago. Moreover, the faience beads from the Harappa site (2600–1900 BC), Pakistan in Indus Valley also contained mixed-alkali and sajji khar (a kind of soda-rich plant ash) (Gu et al. 2016). It is interesting that many of the ornament and pendant sets unearthed in Central China, including Henan (Fig. 2), Shaanxi, and Shanxi provinces, always comprise faience beads and tubes together with carnelian beads that were popular in the Indus Valley, Central Asia, Egypt, and Mesopotamia since the third millennium BC. The generally accepted viewpoint is that the fashion for carnelian beads may have originated from the Indian subcontinent (Aruz and Wallenfels 2003). Rawson (2008) suggested that the sudden emergence of red agate beads in Western Zhou tombs was the consequence of an external stimulus, by comparison with the beads collected in the British Museum from tombs in the Middle East and Central Asia. Since some of the biconical carnelian beads employed in China closely resemble those found in Iran, it is very likely that at least some of them were imported.

During the 2nd millennium BC, there was plenty of mixed-alkali faience from the Southern and Central Europe (Robinson et al. 2004; Henderson 2013). Therefore, the initial mixed-alkali faience objects from Pingdingshan and other regions of Central China were probably imported from the Southern and Central Europe, or the Indus Valley through western China via the ancient Silk Road. Nonetheless, Xinjiang is one of the significant important transfer stations. During this transfer process, some typology and production technologies for faience beads along with carnelian beads were gradually adopted by the ancestors of Western Zhou. Moreover, they had learned to produce faience objects with high potash content, imitating these exotic pieces using local resources (Yang 2020). Furthermore, they extended the technology more widely across Central China and to the surrounding environs. The raw material of alkaline flux used in the potash-dominated faience objects from China was possibly sourced locally in potash-rich plant ashes and minerals (e.g., Niter or Potash feldspar).

## Conclusion

In the present study, the monochrome faience objects unearthed from the cemeteries of Ying and Xu States in Pingdingshan, Henan province, Central China, were analyzed by SEM–EDS, and the alkaline flux types, production technologies, weathering, possible provenances, and exchanges of technology and products were discussed. This study was the first to investigate faience objects that were unearthed from the same region, spanning over a relatively long history (from the early Western Zhou Dynasty to the Spring and Autumn period, about the middle eleventh to middle fifth century BC) in Central China.

It would not be possible to shape the faience objects in a particular style using ground quartz sand and water alone. A glazing mixture, such as alkaline flux, an organic binder, and a Cu-containing colorant material would normally have been applied to the quartz sand body by adjusting the $Na_2O$, $K_2O$, and CuO contents of the interparticle glass within the bodies and the microstructures. However, in some cases, either the alkaline flux or the Cu material was applied to the quartz bodies of some faience objects, probably to facilitate the forming process of the objects and make it more cohesive both before and after firing or to create a blue–green decoration, respectively. The mixture of the volatilized organic binder with the quartz bodies during firing would result in the inner bodies containing several scatters of pores, in contrast to the dense outer interaction layers, particularly for the faience object that was formed without the addition of alkaline flux to its body. Efflorescence and cementation glazing methods are more suitable to the production of small Chinese faience beads and tubes than the direct application glazing method. Due to weathering, the extremely thin glaze layer coated on the surface of faience objects is easily broken; therefore, caution should be exercised in distinguishing the glaze layer from the interaction layer, which depends on the absence or presence of angular quartz particles.

Combining the published results on the faience objects unearthed in Xinjiang, Gansu, Qinghai, Shaanxi, and Shanxi provinces, it was possible to conclude the transition of alkaline flux along with different periods of the Zhou Dynasty (middle eleventh century to middle fifth century BC) and the probable provenances of the faience found in Central China. Only very few soda-rich and potash-rich faience objects, dated to the early Western Zhou Dynasty (1046–977 BC), were found, while many of these two types of faience objects were unearthed in the middle Western Zhou Dynasty (976–878 BC). Since the early Western Zhou Dynasty, the potash-rich faience objects had been produced in Central China, i.e., the Zhou region, and were widely spread across more regions. The soda-rich faience objects that were imported from the West were replaced with mixed-alkali faience objects after the middle Western Zhou Dynasty. All the mixed-alkali faience objects are characterized by a higher potash content than soda; furthermore, perhaps, they have the same provenances as the potash-rich type, some alkali-rich minerals were probably used as the flux agents in these faience objects. However, Eurasian Steppe, Europe, and Indus Valley are not excluded as possible sources of the faience objects in Central China. In any case, Xinjiang is one of the important transfer stations and bridges connecting Central China and the West as well as other foreign areas, such as Egypt, Mesopotamia, Europe, Central Asia, and the Indus Valley for exchanging faience products and technologies via the ancient Silk Road. The transition of alkaline flux used in the faience objects unearthed in Central China is an indication of the variation in the provenances of faience, i.e., from importation to self-production of faience objects using locally available resources. Pingdingshan, which connects eastern and western China, played a significant role in the spread of faience objects from the Western Zhou Dynasty to the Spring and Autumn period. This research will provide some insights into the exchange of technology and the origin of the potash-rich faience unearthed in the Yellow River Basin of China.

**Acknowledgments** We would like to extend our thanks to Ms. Yingzhu Wang, Capital Museum of China; Associate Professor Jian Zhu and Professor Kunlong Chen, University of Science and Technology Beijing; Engineer Qi Gao and Yong Zhang, Shanghai Opton Instrument Co., Ltd.; and Dr. David P. Montgonery for their help in the experimental work and their constructive suggestions.

**Funding** This research was supported by the National Key R&D Program of China (grant number: 2019YFC1520203), the Major Program of National Fund of Philosophy and Social Science of China (grant number: 17ZDA218), and the Humanity and Social Sciences Research Project from the Ministry of Education in China (grant number: 19YJAZH130).

## References

Aruz J, Wallenfels R (2003) Art of the first cities. Metropolitan Museum of Art/Yale University Press, New York, p 279

Brill RH, Martin JH (1991) Scientific research in early Chinese glass. The Corning Museum of Glass, Corning, New York, pp 65–89

Brill RH, Tong SSC, Zhang FK (1989) The chemical composition of a faience bead from China. J Glass Studies 31:11–15

Brill RH, Vocke RD, Wang SX, Zhang FK (1991) A note on lead isotope analysis of faience beads from China. J Glass Studies 33:116–118

Cultural Heritage Bureau of Pingdingshan City, Cultural Heritage Bureau of Ye County (2007) A brief excavation report on the No.4 Tomb of the Spring and Autumn Period at Jiuxian village, Ye County, Henan Province. Cul Relics 9:94–37 (in Chinese)

Dong JQ, Hou DJ, Gan FX (2016) Scientific research on Chinese ancient faience. In: Gan FX (ed) Technological development history of ancient Chinese glasses. Shanghai scientific and technical publishers, Shanghai (in Chinese)

Fu XF, Gan FX (2006) Chinese faience and frit. J Chin Ceram Soc 34: 427–431 (in Chinese)

Gu Z (2015) A study about the relationship between Chinese faience and early glass. Ph. D Thesis Uni Chin Acad Sci (in Chinese)

Gu Z, Kenoyer JM, Yang YY (2016) Investigation of ancient Harappan faience through LA-ICP-AES and SR-μCT. J Instrum 11:C04001

Gu Z, Zhu J, Xie YT, Xiao TQ, Yang YM, Wang CC (2014) Nondestructive analysis of faience beads from the Western Zhou Dynasty, excavated from Peng State cemetery, Shanxi Province, China. J Anal Spectrom 29:1438–1443

Henan Provincial Institute of Cultural Relics and Archaeology, Pingdingshan Administration of Cultural Relics (2012) Cemetery of Ying State in Pingdingshan. Elephant Press, Zhengzhou, pp 1–954 (in Chinese)

Henderson J (1988) Electron probe microanalysis of mixed-alkali glasses. Archaeometry 30:77–91

Henderson J (2013) Ancient glass: an interdisciplinary exploration, Cambridge University Press, pp 183–199

Henderson J, Evans J, Bellintani P, Bietti-Sestieri AM (2015) Production, mixing and provenance of late bronze age mixed alkali glasses from northern Italy: an isotopic approach. J Archaeol Sci 55:1–8

Hou DJ (1987) Study of the origin of Chinese glass from the unearthed cultural relics. Huazhong Archit 3:70–74 (in Chinese)

Jiang LJ, Luo YX, Zhao J, Zhuang TG (2008) Hepatic CT image retrieval based on the combination of Gabor filters and support vector machine. Chin Opt Lett 6(7):495–498

Kiefer C, Allibert A (1971) Pharaonoic blue ceramics: the process of self-glazing. Archaeology 24:107–117

Lei Y, Xia Y (2015) Study on production techniques and provenance of faience beads excavated in China. J Archaeol Sci 53:32–42

Li QH, Dong JQ, Gan FX (2009) Research and discussion on chemical composition and technics of the early faience and glass artifacts unearthed from China. J Guangxi Univ Nat (Nat Sci Ed) 15(4):1–41 (in Chinese)

Lin YX, Rehren T (2017) Investigation on faience beads from Yanyuan collected in Liangshan Museum. Sichuan Cul Relics 6:60–71 (in Chinese)

Lin YX, Rehren T, Wang H, Ren XY, Ma J (2019) The beginning of faience in China: a review and new evidence. J Archaeol Sci 105: 97–115

Liu N, Yang YM, Wang YQ, Hu WL, Jiang XCY, Ren M, Yang M, Wang CS (2017) Nondestructive characterization of ancient faience beads unearthed from Ya'er cemetery in Xinjiang, Early Iron Age China. Ceram Int 43:10460–10467

Liu S, Li QH, Gan FX, Zhang P (2011) Characterization of some ancient glass vessels fragments found in Xinjiang, China, using a portable energy dispersive XRF spectrometer. X-Ray Spectrom 40(5):364–375

Liu Y, Wang YZ, Chen KL, Mei JJ, Ma HJ, L CX, Zhu L, Xie YT (2019) Scientific analysis of the faience unearthed from the tomb of M6043 at the Dahekou Cemetery in Yicheng County, Shanxi Province. Archaeol Cult Relics 2:116–121 (in Chinese)

Qin Y, Chen X, Li XL, Chen QW (2012) Analysis and imitations of manufacture technique on quartz bead (faience) from Zengguo tomb of Guojiamiao, Zaoyang. J Chin Ceram Soc 40(4):567–576 (in Chinese)

Rawson J (2008) In search of ancient red beads and carved jade in modern China. Cabiersd' Extrême—Asie 17:10–11

Robinson C, Baczyńska B, Polańska M (2004) The origins of faience in Poland. Sprawozdania Archeol 56:79–121

Shortland AJ, Tite MS (2005) Technological study of Ptolemaic–early Roman faience from Memphis, Egypt. Archaeometry 47:31–46

Tite MS, Bimson M (1986) Faience: an investigation of the microstructures associated with the different methods of glazing. Archaeometry 28:69–78

Tite MS, Frestone IC, Bimson M (1983) Egyptian faience: an investigation of the methods production. Achaeometry 25:17–27

Tite MS, Shortland AJ (2008) Production technology of faience and related early viteous materials. Oxford University School of Archaeology, Oxford, pp 1–109

Vandiver PB (2008) Raw materials and fabrication methods used in the production of faience. In: Tite MS, Shortland AJ (eds) Production technology of faience and related early vitreous materials. Oxford School of Archaeology, Oxford, pp 37–55

Wang SX (1986) Identification and research of the pristine glass from Zhouyuan, Shaanxi province dated to Western Zhou Dynasty. Relics Museol 2:26–30 (in Chinese)

Wang YZ (2019). The technological research of faience in Western-Zhou and eastern-Zhou periods. Ph. D Thesis, Uni Sci Technol Beijing (in Chinese)

Wang YZ, Chen KL, Ma QL, Ma HJ, Zhagn ZG, Jiang T (2017) The analysis of faience beads from Marquis Guo State Cemetery in Sanmen Gorge of Henan Province. Sci Conser Archaeol 29(2):45–54

Wang YZ, Rehren T, Tan YC, Cong DX, Jia PWM, Hendersong J, Ma HJ, Betts A, Chen KL (2020) New evidence for the transcontinental spread of early faience. J Archaeol Sci 116:1–8

Wulff HE, Wulff HS, Koch L (1968) Egyptian faience: a possible survival in Iran. Archaeology 21:98–107

Xia KY, Zhai XH, Xie ZH, Zhou K, Feng YT, Zhang GJ, Li CH (2018) Dual-modal photoacoustic/CT imaging system. Chin Opt Lett 16(12):121701

Yang YM (2020) Archaeometry should be based on archaeology. A comment on Lin et al. J Archaeol Sci 119:105149

Zhang W (2003) Study of bronze culture in Qinghai region. Ph. D Thesis, Jilin University. (in Chinese)

Zhang W (2009) A query about the viewpoint of the periods of bronzes in the Kayao culture. Res Chin Front Archaeolo 8:74–80 (in Chinese)

Zhang ZY, Xu Y, Zhang BZ (2015) SEM observation and Raman analysis on 6H-SiC wafer damage irradiated by nanosecond pulsed Nd : YAG laser. Chin Opt Lett 13(z1):S12203–S312206

Zhao HX, Cheng HS, Li QH, Gan FX (2011) Nondestructive identification of ancient Chinese glasses by Raman and proton-induced X-ray emission spectroscopy. Chin Opt Lett 9(03):033001–033004